ACS OMEGA

Open Access



http://pubs.acs.org/journal/acsodf

Article

# Determination and Correlation of Solubility of *N*-Acetylglucosamine in Four Aqueous Binary Solvents from 283.15 to 323.15 K

Xiaoyu Cao, Yan Wang, Jianxing Lu, Qian Zhang, Tao Yuan, Shichao Du,* and Fumin Xue*

Cite This: *ACS Omega* 2023, 8, 47463−47471

Read Online

ACCESS | Metrics & More | Article Recommendations | Supporting Information

**ABSTRACT:** *N*-Acetylglucosamine (NAG) is a significant novel functional monosaccharide with a wide range of potential applications, such as in the medical and cosmetic fields. A gravimetric technique was used to assess the solubility of NAG in water, methanol, *N*,*N*-dimethylformamide, water + methanol, water + *n*-propanol, water + *N*,*N*-dimethylformamide, and water + acetonitrile at temperatures ranging from 283.15 to 323.15 K. The outcomes of the experiment demonstrated that the temperature and water content were positively correlated with the solubility of NAG in four experimental binary solvents. The order of solubility in the four aqueous solvent mixtures is water + DMF > water + methanol > water + *n*-propanol > water + acetonitrile. The solubility data was well correlated using the modified Apelblat model, the CNIBS/R-K model, and the Apelblat−Jouyban−Acree model. Experimental data from NAG will help guide the design of cooling and dissolution in crystallization processes.

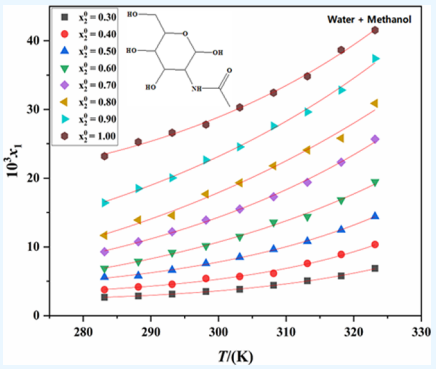


## 1. INTRODUCTION

*N*-Acetylglucosamine (NAG, $C_8H_{15}NO_6$, CAS registry number: 7512-17-6, Figure 1) is a kind of amino monosaccharide in which the hydroxyl group on the second position C of the glucose molecule is replaced by an acetylamino group. Typically, it comes as a white powder with a somewhat pleasant flavor.[1] NAG is the monomer unit of chitin and the basic component of hyaluronic acid on the cell surface.[2] It can be employed for immunomodulation and biosynthesis, among other things.[3,4] NAG can also inhibit the metastasis of cancer cells at a certain concentration, thus improving the resistance of the human body to cancer cells.[5] Huang et al. showed that NAG has a good effect in the treatment of gastric cancer.[6] In addition to being widely utilized in medicine, they also make excellent additions to cosmetics and healthcare items.[7]

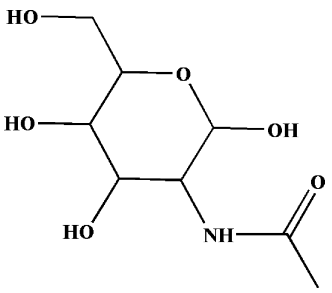


**Figure 1.** Chemical structure of NAG.

A few NAG reports have already been made public.[8,9] But the current studies on NAG's solubility are not as prevalent as research on its applications in different fields. Hesketh et al. found that oral NAG can alter the insulin content, which proves that it may play a certain role in the treatment of diabetes.[10] NAG also has great potential application value in the cosmetics industry. It is a suitable substrate for the synthesis of hyaluronic acid, which can accelerate the synthesis of collagen in cells and delay cell senescence.[11]

The study of crystal thermodynamics serves as the basis for understanding crystallization kinetics and processes.[12] Solubility measurement is the cornerstone of crystal thermodynamic research. In view of the current research progress of NAG, we measured the solubility of NAG in water, methanol, *N*,*N*-dimethylformamide, water + methanol, water + *n*-propanol, water + DMF, and water + acetonitrile at 283.15−323.15 K by gravimetric methods. In addition to being miscible with water, the four organic solvents were chosen because NAG is much more soluble in water than in the other three. The solubility data of NAG in certain solvent systems can guide the design of the solvation crystals. We determined the solubility of NAG in three pure solvents (water, methanol, and *N*,*N*-dimethylformamide) and four binary mixed solvents. Using water as a good solvent and selecting four commonly used antisolvents to form four groups of binary mixed solvents (water + methanol, water + *n*-

**Received:** June 8, 2023
**Revised:** September 12, 2023
**Accepted:** November 16, 2023
**Published:** December 4, 2023

Table 1. Details of the Material Specification[a,b]

| materials | CAS no. | molar mass(g·mol$^{-1}$) | source | mass fraction purity | analysis method |
|---|---|---|---|---|---|
| *N*-acetylglucosamine | 7512-17-6 | 221.208 | Shandong Runde Biotechnology Co., Ltd. | ≥0.998 | GC[c] |
| methanol | 67-56-1 | 32.04 | Sinopharm Chemical Reagent Co., Ltd. | ≥0.997 | GC[c] |
| *n*-propanol | 71-23-8 | 60.1 | Sinopharm Chemical Reagent Co., Ltd. | ≥0.995 | GC[c] |
| *N*,*N*-dimethylformamide | 67-63-0 | 73.095 | Sinopharm Chemical Reagent Co., Ltd. | ≥0.997 | GC[c] |
| acetonitrile | 75-05-8 | 41.052 | Sinopharm Chemical Reagent Co., Ltd. | ≥0.998 | GC[c] |

[a]Both the analysis method and mass fraction purity were provided by suppliers. [b]High-performance liquid chromatography. [c]Gas chromatography.

propanol, water + DMF, and water + acetonitrile), the solubility test was conducted at 278.15−318.15 K. Methanol, *n*-propanol, DMF, and acetonitrile are common and widely used solvents. Studying the solubility of NAG in these four mixed solvents has practical application significance. To expand the application scope, the modified Apelblat model,[13] the CNIBS/R-K model,[14] and the Apelblat−Jouyban−Acree model[15] were used to correlate the data.

## 2. EXPERIMENTAL SECTION

**2.1. Materials.** NAG (CAS no. 7512-17-6) was supplied by Shandong Runde Biotechnology Co. Ltd. The solvents used in this study (methanol, *n*-propanol, and acetonitrile) were purchased from Sinopharm Chemical Reagent Co., Ltd., China. *N*,*N*-Dimethylformamide was purchased from Tianjin Fuyu Fine Chemical Co., Ltd. The deionized water was prepared in the laboratory (Arium Mini Plus, Germany). All organic solvents were of analytical grade and used without repurification. Details of the materials used in these experiments are listed in Table 1. The purity and purity analysis methods were provided by the supplier.

**2.2. Solubility Measurement.** The solubility of NAG in three pure solvents and four binary solvents was determined by the gravimetric method in the temperature range of 283.15−323.15 K. The experimental procedures were as follows. (1) Excess of solid NAG was dissolved in 30 g of binary solvent and placed in a 100 mL glass tube, which was placed in a double-layer jacket glass container. A glass container was attached to a constant temperature bath (CF41, Junlabo, Germany) to control the system temperature difference within ±0.05 K. The solution was stirred for 12 h using a magnetic stirring device (MS-H-S type, DLAB Scientific Co., Ltd., China). No dissolution of the NAG after 12 h could determine whether the system had reached solid−liquid equilibrium. (2) After turning off the stirring, the solution was allowed to stand for 2 h. The filtered supernatant was weighed immediately after being injected into a preweighed Petri dish using a preheated/precooled 5 mL syringe and a 0.45 $\mu$m filter membrane. (3) The Petri dish was put in a vacuum drying oven (DZF-6000, Shanghai Yiheng Scientific Instrument Co., Ltd., China) at 323.15 K for at least 12 h, until the mass was constant. The mass of the samples was analyzed by analytical balances (ME type, Mettler Toledo, Switzerland) with a precision of ±0.0001 g. The solubility was calculated by using the average of the data after three repeated measurements for each experiment to reduce experimental error. The content ratio of water ($x_2^0$) in the initial binary solvent and the mole fraction solubility ($x_1$) of NAG in binary solvents was calculated using eqs 1 and 2.

$$x_2^0 = \frac{m_2/M_2}{m_2/M_2 + m_3/M_3} \tag{1}$$

$$x_1 = \frac{m_1/M_1}{m_1/M_1 + m_2/M_2 + m_3/M_3} \tag{2}$$

where $m_1$ represents the mass of NAG and $m_2$ and $m_3$ are the masses of water and organic solvent, respectively. $M_1$, $M_2$, and $M_3$ are molecular masses of NAG, water, and organic solvent, respectively.

**2.3. X-ray Powder Diffraction.** X-ray diffraction (PXRD) was used to confirm the crystal form of NAG in the experimental temperature range, and it was found that there was no change in the crystallographic structure of NAG. X'Pert[3] powder diffractometer (MiniFlex600, Rigaku, Japan) was used. During the measurement, the tube voltage and current were set at 40 kV and 30 mA. EMPYREAN (PANalytical, The Netherlands) collected two ranges of Cu K$\alpha$ radiation (0.15405 nm) at room temperature in order to measure these patterns. The scan rate was 8°/min, and the step size was 0.02°.

**2.4. Thermal Examination.** The thermal gravimetric analyzer-differential scanning calorimetry (TGA-DSC) method was used to determine the melting parameters of NAG. The melting temperature $T_m$ and the enthalpy of melting $\Delta H_{fus}$ of NAG were determined by TGA and DSC (TGA/DSC 3+, METTLER TOLEDO, Switzerland). Approximately 5−10 mg of NAG was added to the aluminum crucible. Nitrogen was used as a protective gas, and a heating rate of 10 K/min was used to assess the NAG's melting properties.

## 3. THERMODYNAMIC MODELS

**3.1. Modified Apelblat Equation.** The modified Apelblat equation is an accurate semiempirical equation.[16] It is commonly used to correlate solubility at different temperatures.[17−19] It is represented by the following eq 3.

$$\ln x_1 = A + \frac{B}{T/\mathrm{K}} + C\ln(T/\mathrm{K}) \tag{3}$$

where $x_1$ represents the mole fraction solubility; $T$ represents the selected test temperature; and $A$, $B$, and $C$ are empirical constants. $A$ and $B$ parameters represent the change in activity coefficient in solution, and $C$ represents how melting enthalpy is affected by temperature.[20]

**3.2. CNIBS/R-K Model.** The CNIBS/R-K model may be used to illustrate the link between the solvent composition and the isothermal mole fraction solubility of a binary solvent combination.[21−23] The expression is shown in eq 4.

$$\ln x_1 = x_2^0 \ln x_A + x_3^0 \ln x_B + x_2^0 x_3^0 \sum_{i=0}^{n} S_i (x_2^0 - x_3^0)^i \tag{4}$$

where $x_1$ is the solute's mole fraction solubility. The saturated mole solubilities of the solute in the respective pure solvents are denoted by the letters $x_A$ and $x_B$. The starting mole percentages of the solvent mixture are $x_2^0$ and $x_3^0$. The parameters of the model



https://doi.org/10.1021/acsomega.3c04044
ACS Omega 2023, 8, 47463−47471

are $S_i$ and $n$. In binary solvent mixtures, eq 4 can be simplified to eq 5.

$$\ln x_1 = x_2^0 \ln x_A + (1 - x_2^0)\ln x_B + (1 - x_2^0)x_2^0 + [S_0 + S_1(2x_2^0 - 1) + S_2(2x_2^0 - 1)^2] \quad (5)$$

We used $b_1$−$b_5$ to replace the constant parameters ineq 5. Eq 5 can be expressed as eq 6.

$$\ln x_1 = b_1 + b_2 x_2^0 + b_3(x_2^0)^2 + b_4(x_2^0)^3 + b_5(x_2^0)^4 \quad (6)$$

**3.3. Apelblat−Jouyban−Acree Model.** The Apelblat−Jouyban−Acree model may be used to represent the connection between composition of solvent and temperature in a variety of solvents;[24] and the expression is shown in eq 7.

$$\ln x_1 = x_2^0 \ln x_A + x_3^0 \ln x_B + x_2^0 x_3^0 \sum_{i=0}^{n} \frac{J_i(x_2^0 - x_3^0)^i}{T} \quad (7)$$

where $x_2^0$ and $x_3^0$ stand for the binary solvent mixture's initial molecular fraction makeup when the solute was not added.[25] $J_i$ is the model constant, and $x_A$ and $x_B$ stand for the mole solubility of the solute in pure solvent. In binary mixed solvents, eq 7 can be simplified to eq 8.

$$\ln x_1 = a_3 + b_3/T + c_3 \ln T + (a_2 - a_3)x_2^0 + (b_2 - b_3 + J_0 - J_1 + J_2)\frac{x_2^0}{T} + (3J_1 - J_0 - 5J_2)\frac{(x_2^0)^2}{T} + (8J_2 - 2J_1)\frac{(x_2^0)^3}{T} + (-4J_2)\frac{(x_2^0)^4}{T} + (C_2 - C_3)x_2^0 \ln T \quad (8)$$

We used $A_0$−$A_8$ to replace the constant parameters in eq 8. Eq 8 can be expressed as eq 9.

$$\ln x_1 = A_0 + \frac{A_1}{T} + A_2 \ln T + A_3 x_2^0 + A_4 \frac{x_2^0}{T} + A_5 \frac{(x_2^0)^2}{T} + A_6 \frac{(x_2^0)^3}{T} + A_7 \frac{(x_2^0)^4}{T} + A_8 x_2^0 \ln T \quad (9)$$

To evaluate the accuracy of the model, the average relative deviation (ARD %) and root-mean-square deviation (RMSD) are computed.[26,27] The expressions are shown in eqs 10 and 11.

$$\mathrm{ARD\%} = \frac{100}{n} \sum_{i=1}^{n} \left| \frac{x_i^{exp} - x_i^{cal}}{x_i^{exp}} \right| \quad (10)$$

$$\mathrm{RMSD} = \sqrt{\frac{\sum_{i=1}^{n} (x_i^{cal} - x_i^{exp})^2}{n}} \quad (11)$$

where $x_i^{exp}$ and $x_i^{cal}$refer to the experimental mole fraction solubility and calculated mole fraction solubility of NAG, and $n$ stands for the number of experimental data points.

## 4. RESULTS AND DISCUSSION

**4.1. Characterization of NAG.** The crystal forms of NAG were detected by PXRD. The remaining solids were tested after shaking the crystals in four solvents, such as water + methanol, water + *n*-propanol, water + DMF, and water + acetonitrile for 12 h. The experimental results are listed in Figure 2. The peaks of the PXRD spectrum are mainly at 9.98, 19.78, 27.52, and 30.76°. The characteristic diffraction peaks have not changed, which indicates that there is no crystal-form transition in the whole experiment.

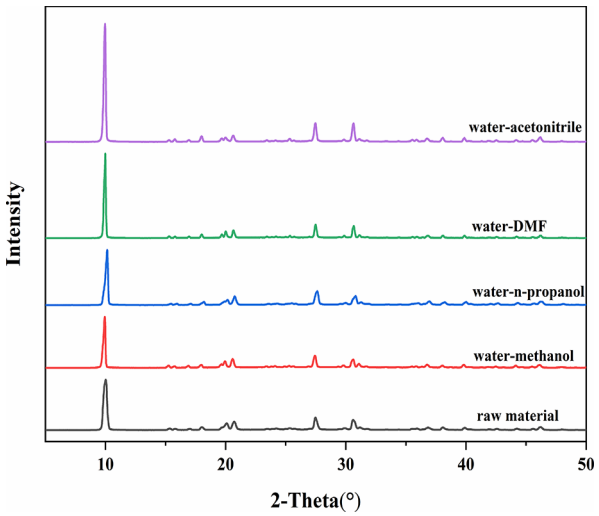


**Figure 2.** PXRD patterns of raw material and residual solids of NAG in aqueous binary solvent mixtures.

The results of TGA and DSC analyses of NAG are presented in Figure 3. The graphic shows that the initial melting temperature is approximately 482.28 K. It indicates that the NAG is well stabilized throughout the experiment.

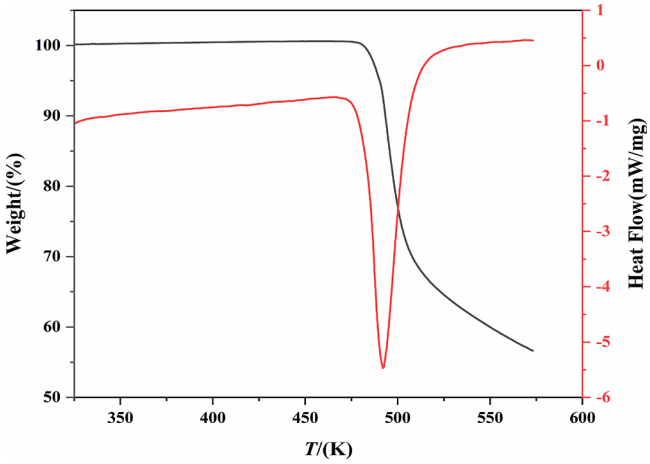


**Figure 3.** TGA and DSC plots of NAG.

**4.2. Solubility of NAG.** All the solubility data obtained in this work are shown in Tables 2−5 and plotted in Figures S1−S8. As shown in the table and figure, the solubility of NAG in a combination of four binary solvents increased with increasing temperature (283.15−323.15 K) or molar amount of water (0−1).

The mole fraction solubility of NAG in the same solvent system is positively correlated with temperature. At the same temperature, the order of solubility in four binary solvent mixtures is water + DMF > water + methanol > water + *n*-propanol > water + acetonitrile.

The interactions between solvent and solute molecules, such as hydrogen bonds and van der Waals forces, are typically connected to solubility. In our research setup, NAG is a polar



https://doi.org/10.1021/acsomega.3c04044
ACS Omega 2023, 8, 47463−47471

Table 2. Experimental and Correlated Solubility of NAG in Water + Methanol at Temperatures from 283.15 to 323.15 K under Atmospheric Pressure ($p$ = 0.1 MPa)[a,b]

| $x_2^0$ | $10^3x_1^{exp}$ | $10^3x_1^{Apelblat}$ | $10^3x_1^{CNIBS}$ | $10^3x_1^{AJA}$ |
|---|---|---|---|---|
| | | 283.15 K | | |
| 0.00 | 0.6835 | 0.6599 | 0.6833 | 0.6382 |
| 0.30 | 2.678 | 2.675 | 2.669 | 2.533 |
| 0.40 | 3.768 | 3.828 | 3.868 | 3.819 |
| 0.50 | 5.600 | 5.455 | 5.340 | 5.511 |
| 0.60 | 6.868 | 6.929 | 7.085 | 7.594 |
| 0.70 | 9.298 | 9.422 | 9.185 | 10.03 |
| 0.80 | 11.68 | 11.83 | 11.93 | 12.85 |
| 0.90 | 16.42 | 16.56 | 16.06 | 16.20 |
| 1.00 | 23.20 | 23.49 | 23.36 | 20.60 |
| | | 288.15 K | | |
| 0.00 | 0.7080 | 0.7233 | 0.7081 | 0.7033 |
| 0.30 | 2.857 | 2.873 | 2.858 | 2.782 |
| 0.40 | 4.184 | 4.151 | 4.161 | 4.193 |
| 0.50 | 5.790 | 6.011 | 5.834 | 6.053 |
| 0.60 | 7.886 | 7.892 | 7.938 | 8.352 |
| 0.70 | 10.75 | 10.67 | 10.58 | 11.06 |
| 0.80 | 13.91 | 13.43 | 13.98 | 14.19 |
| 0.90 | 18.49 | 18.29 | 18.57 | 17.95 |
| 1.00 | 25.26 | 24.82 | 25.20 | 22.88 |
| | | 293.15 K | | |
| 0.00 | 0.7807 | 0.8028 | 0.7814 | 0.7877 |
| 0.30 | 3.135 | 3.133 | 3.090 | 3.089 |
| 0.40 | 4.557 | 4.564 | 4.654 | 4.646 |
| 0.50 | 6.626 | 6.677 | 6.666 | 6.698 |
| 0.60 | 9.190 | 8.981 | 9.080 | 9.236 |
| 0.70 | 12.20 | 12.08 | 11.87 | 12.23 |
| 0.80 | 14.59 | 15.20 | 15.21 | 15.71 |
| 0.90 | 20.04 | 20.20 | 19.66 | 19.88 |
| 1.00 | 26.61 | 26.37 | 26.68 | 25.36 |
| | | 298.15 K | | |
| 0.00 | 0.8913 | 0.9048 | 0.8905 | 0.8957 |
| 0.30 | 3.515 | 3.464 | 3.567 | 3.464 |
| 0.40 | 5.401 | 5.084 | 5.289 | 5.192 |
| 0.50 | 7.601 | 7.473 | 7.549 | 7.462 |
| 0.60 | 10.15 | 10.21 | 10.38 | 10.27 |
| 0.70 | 13.90 | 13.68 | 13.79 | 13.57 |
| 0.80 | 17.68 | 17.14 | 17.78 | 17.41 |
| 0.90 | 22.65 | 22.32 | 22.43 | 22.02 |
| 1.00 | 27.79 | 28.15 | 27.90 | 28.07 |
| | | 303.15 K | | |
| 0.00 | 1.023 | 1.033 | 1.023 | 1.033 |
| 0.30 | 3.828 | 3.880 | 3.812 | 3.923 |
| 0.40 | 5.699 | 5.733 | 5.768 | 5.848 |
| 0.50 | 8.492 | 8.422 | 8.377 | 8.367 |
| 0.60 | 11.50 | 11.60 | 11.61 | 11.47 |
| 0.70 | 15.51 | 15.48 | 15.36 | 15.11 |
| 0.80 | 19.32 | 19.27 | 19.56 | 19.33 |
| 0.90 | 24.55 | 24.66 | 24.36 | 24.39 |
| 1.00 | 30.29 | 30.20 | 30.34 | 31.00 |
| | | 308.15 K | | |
| 0.00 | 1.223 | 1.195 | 1.225 | 1.207 |
| 0.30 | 4.417 | 4.399 | 4.301 | 4.482 |
| 0.40 | 6.152 | 6.538 | 6.494 | 6.635 |
| 0.50 | 9.637 | 9.553 | 9.465 | 9.436 |
| 0.60 | 13.59 | 13.17 | 13.19 | 12.86 |
| 0.70 | 17.30 | 17.51 | 17.51 | 16.87 |
| 0.80 | 21.79 | 21.61 | 22.21 | 21.49 |
| 0.90 | 27.57 | 27.26 | 27.16 | 27.01 |
| 1.00 | 32.43 | 32.53 | 32.52 | 34.19 |
| | | 313.15 K | | |
| 0.00 | 1.481 | 1.397 | 1.481 | 1.427 |
| 0.30 | 5.071 | 5.043 | 5.110 | 5.161 |
| 0.40 | 7.596 | 7.534 | 7.524 | 7.581 |
| 0.50 | 10.81 | 10.90 | 10.71 | 10.70 |
| 0.60 | 14.39 | 14.93 | 14.66 | 14.49 |
| 0.70 | 19.40 | 19.80 | 19.23 | 18.89 |
| 0.80 | 24.10 | 24.15 | 24.22 | 23.93 |
| 0.90 | 29.62 | 30.12 | 29.45 | 29.90 |
| 1.00 | 34.83 | 35.18 | 34.91 | 37.64 |
| | | 318.15 K | | |
| 0.00 | 1.643 | 1.651 | 1.642 | 1.706 |
| 0.30 | 5.767 | 5.842 | 5.820 | 5.990 |
| 0.40 | 8.902 | 8.768 | 8.754 | 8.715 |
| 0.50 | 12.47 | 12.51 | 12.55 | 12.20 |
| 0.60 | 16.82 | 16.92 | 17.00 | 16.38 |
| 0.70 | 22.32 | 22.38 | 21.77 | 21.20 |
| 0.80 | 25.81 | 26.92 | 26.70 | 26.66 |
| 0.90 | 32.82 | 33.29 | 32.04 | 33.10 |
| 1.00 | 38.64 | 38.19 | 38.88 | 41.37 |
| | | 323.15 K | | |
| 0.00 | 1.915 | 1.970 | 1.914 | 2.062 |
| 0.30 | 6.882 | 6.834 | 6.936 | 7.000 |
| 0.40 | 10.34 | 10.30 | 10.21 | 10.08 |
| 0.50 | 14.43 | 14.43 | 14.47 | 13.97 |
| 0.60 | 19.47 | 19.15 | 19.63 | 18.58 |
| 0.70 | 25.68 | 25.28 | 25.41 | 23.84 |
| 0.80 | 30.88 | 29.93 | 31.35 | 29.74 |
| 0.90 | 37.39 | 36.78 | 36.93 | 36.62 |
| 1.00 | 41.53 | 41.59 | 41.69 | 45.41 |

[a] $x_1$ is the experimental solubility; $x_1^{Apelblat}$, $x_1^{CNIBS}$, and $x_1^{AJA}$ are the calculated mole solubility according to the modified Apelblat model, the CNIBS/R-K model, and the Apelblat−Jouyban−Acree model, respectively. $x_2^0$ represents the initial mole fraction of water in the binary aqueous solvent. [b] The standard uncertainty is $u(T)$= 0.1 K, and the relative standard uncertainties $u_r$ are $u_r(P)$ = 0.01, $u_r(x_1)$ = 0.02, and $u_r(x_2^0)$ = 0.001.

molecule. Water, methanol, *n*-propanol, and DMF are polar protic solvents; the order of polarity is water (1.09) > DMF (0.88) > methanol (0.60) > *n*-propanol (0.52), and acetonitrile is a polar aprotic solvent. The main physicochemical properties of the five pure solvents are given in Table 6. According to the data in the table, it can be concluded that the dissolution order of NAG in binary solvent is the same as the sum of hydrogen bond donor tendencies of pure solvent, indicating that hydrogen bonding plays an important role. In other words, the solubility order is positively associated with polarity, except for the water + acetonitrile solvent system. The C═O group in DMF solvent can interact with the N−H group of NAG molecules, enhancing the solubility of NAG. O−H bonds in alcohol solvents have negligible interaction with NAG. In summary, polarity has a significant impact on how soluble NAG is in mixed solvents.

**4.3. Data Correlation.** To expand the application range of solubility data, we linked the experimental data to three thermodynamic models. The parameters, ARD, and RMSD



https://doi.org/10.1021/acsomega.3c04044
ACS Omega 2023, 8, 47463−47471

Table 3. Experimental and Correlated Solubility of NAG in Water + *N*-Propanol at Temperatures from 283.15 to 323.15 K under Atmospheric Pressure ($p$ = 0.1 MPa)[a,b]

| $x_2^0$ | $10^3x_1^{exp}$ | $10^3x_1^{Apelblat}$ | $10^3x_1^{CNIBS}$ | $10^3x_1^{AJA}$ |
|---|---|---|---|---|
| 283.15 K | | | | |
| 0.30 | 0.6709 | 0.6910 | 0.6852 | 0.6379 |
| 0.40 | 1.371 | 1.405 | 1.282 | 1.350 |
| 0.50 | 2.378 | 2.455 | 2.463 | 2.661 |
| 0.60 | 4.139 | 4.177 | 4.516 | 4.795 |
| 0.70 | 8.402 | 8.256 | 7.584 | 7.850 |
| 0.80 | 11.65 | 11.63 | 11.56 | 11.73 |
| 0.90 | 15.55 | 15.64 | 16.37 | 16.28 |
| 1.00 | 23.20 | 23.49 | 22.78 | 21.57 |
| 288.15 K | | | | |
| 0.30 | 0.8857 | 0.8480 | 0.8887 | 0.8005 |
| 0.40 | 1.773 | 1.656 | 1.759 | 1.652 |
| 0.50 | 3.269 | 3.059 | 3.249 | 3.179 |
| 0.60 | 5.372 | 5.238 | 5.534 | 5.602 |
| 0.70 | 8.876 | 9.108 | 8.697 | 8.983 |
| 0.80 | 12.91 | 13.01 | 12.77 | 13.17 |
| 0.90 | 17.66 | 17.53 | 17.96 | 17.95 |
| 1.00 | 25.26 | 24.82 | 25.12 | 23.39 |
| 293.15 K | | | | |
| 0.30 | 0.9720 | 1.018 | 0.9683 | 0.9824 |
| 0.40 | 1.855 | 1.940 | 1.885 | 1.984 |
| 0.50 | 3.688 | 3.717 | 3.600 | 3.743 |
| 0.60 | 6.283 | 6.386 | 6.360 | 6.475 |
| 0.70 | 10.08 | 10.09 | 10.12 | 10.21 |
| 0.80 | 14.63 | 14.53 | 14.57 | 14.73 |
| 0.90 | 19.67 | 19.58 | 19.66 | 19.80 |
| 1.00 | 26.61 | 26.37 | 26.62 | 25.45 |
| 298.15 K | | | | |
| 0.30 | 1.303 | 1.197 | 1.296 | 1.181 |
| 0.40 | 2.335 | 2.261 | 2.378 | 2.343 |
| 0.50 | 4.390 | 4.414 | 4.345 | 4.346 |
| 0.60 | 7.606 | 7.583 | 7.440 | 7.406 |
| 0.70 | 11.28 | 11.23 | 11.57 | 11.52 |
| 0.80 | 16.25 | 16.22 | 16.32 | 16.43 |
| 0.90 | 21.79 | 21.83 | 21.47 | 21.83 |
| 1.00 | 27.79 | 28.15 | 27.93 | 27.78 |
| 303.15 K | | | | |
| 0.30 | 1.410 | 1.381 | 1.397 | 1.391 |
| 0.40 | 2.575 | 2.621 | 2.657 | 2.722 |
| 0.50 | 5.049 | 5.129 | 4.941 | 4.982 |
| 0.60 | 8.727 | 8.785 | 8.487 | 8.390 |
| 0.70 | 12.65 | 12.54 | 13.11 | 12.91 |
| 0.80 | 18.12 | 18.09 | 18.26 | 18.25 |
| 0.90 | 24.28 | 24.28 | 23.71 | 24.07 |
| 1.00 | 30.29 | 30.20 | 30.53 | 30.42 |
| 308.15 K | | | | |
| 0.30 | 1.555 | 1.564 | 1.538 | 1.609 |
| 0.40 | 2.912 | 3.025 | 3.014 | 3.113 |
| 0.50 | 5.744 | 5.839 | 5.617 | 5.642 |
| 0.60 | 9.908 | 9.944 | 9.575 | 9.418 |
| 0.70 | 14.07 | 14.06 | 14.67 | 14.39 |
| 0.80 | 20.11 | 20.15 | 20.30 | 20.22 |
| 0.90 | 26.80 | 26.94 | 26.08 | 26.54 |
| 1.00 | 32.43 | 32.53 | 32.73 | 33.41 |
| 313.15 K | | | | |
| 0.30 | 1.654 | 1.742 | 1.652 | 1.829 |
| 0.40 | 3.672 | 3.474 | 3.670 | 3.510 |
| 0.50 | 6.611 | 6.521 | 6.727 | 6.316 |
| 0.60 | 11.24 | 11.01 | 10.86 | 10.48 |
| 0.70 | 15.79 | 15.80 | 16.11 | 15.94 |
| 0.80 | 22.22 | 22.44 | 22.43 | 22.34 |
| 0.90 | 29.69 | 29.83 | 29.27 | 29.26 |
| 1.00 | 34.83 | 35.18 | 34.97 | 36.78 |
| 318.15 K | | | | |
| 0.30 | 1.802 | 1.908 | 1.801 | 2.046 |
| 0.40 | 3.949 | 3.972 | 3.957 | 3.904 |
| 0.50 | 7.255 | 7.152 | 7.241 | 6.994 |
| 0.60 | 11.80 | 11.95 | 11.80 | 11.57 |
| 0.70 | 17.83 | 17.82 | 17.81 | 17.57 |
| 0.80 | 25.16 | 24.97 | 25.25 | 24.60 |
| 0.90 | 33.25 | 32.97 | 33.15 | 32.25 |
| 1.00 | 38.64 | 38.19 | 38.67 | 40.58 |
| 323.15 K | | | | |
| 0.30 | 2.228 | 2.059 | 2.239 | 2.253 |
| 0.40 | 4.496 | 4.523 | 4.411 | 4.287 |
| 0.50 | 7.659 | 7.713 | 7.818 | 7.666 |
| 0.60 | 12.75 | 12.72 | 12.82 | 12.67 |
| 0.70 | 20.08 | 20.14 | 19.65 | 19.26 |
| 0.80 | 27.76 | 27.76 | 28.02 | 27.03 |
| 0.90 | 36.31 | 36.36 | 36.40 | 35.53 |
| 1.00 | 41.53 | 41.59 | 41.46 | 44.88 |

[a] $x_1$ is the experimental solubility; $x_1^{Apelblat}$, $x_1^{CNIBS}$, and $x_1^{AJA}$ are the calculated mole solubility according to the modified Apelblat model, the CNIBS/R-K model, and the Apelblat−Jouyban−Acree model, respectively. $x_2^0$ represents the initial mole fraction of water in the binary aqueous solvent. [b] The standard uncertainty is $u(T)$= 0.1 K, and the relative standard uncertainties $u_r$ are $u_r(P)$ = 0.01, $u_r(x_1)$ = 0.03, and $u_r(x_2^0)$ = 0.001.

data of the selected models are shown in Tables S1−S3. All of the ARD % values are smaller than 5.97%, proving that these models can accurately predict the solubility data. For water + methanol, the fitting order of the selected three thermodynamic models is Apelblat−Jouyban−Acree model (ARD = 0.0319) > CNIBS/R-K model (ARD = 0.0155) > modified Apelblat model (ARD = 0.0150). In addition, the correlation ability of *F*-test evaluation model for data is shown in Table S4. The results of *F*-test and ARD judgment are consistent; the fitting effect of modified Apelblat model parameters is the best. For water + *n*-propanol, the fitting order is Apelblat−Jouyban−Acree model (ARD = 0.0355) > CNIBS/R-K model (ARD = 0.0212) > modified Apelblat model (ARD = 0.0168). For water + DMF, the fitting order is Apelblat−Jouyban−Acree model (ARD = 0.0436) > CNIBS/R-K model (ARD = 0.0142) > modified Apelblat model (ARD = 0.0127). For water + acetonitrile, the fitting order is Apelblat−Jouyban−Acree model (ARD = 0.0355) > CNIBS/R-K model (ARD = 0.0212) > modified Apelblat model (ARD = 0.0199).

The findings demonstrate that all three thermodynamic models used in this work give good-fitting results. The modified Apelblat model can correlate the solubility data at various temperatures, whereas the CNIBS/R-K model can correlate the solubility of various binary solvents with various compositions, and the Apelblat−Jouyban−Acree model can also take temperature and solvent content into account. According to the fitting



https://doi.org/10.1021/acsomega.3c04044
ACS Omega 2023, 8, 47463−47471

Table 4. Experimental and Correlated Solubility of NAG in Water + *N*,*N*-Dimethylformamide at Temperatures from 283.15 to 323.15 K under Atmospheric Pressure ($p$ = 0.1 MPa)[a,b]

| $x_2^0$ | $10^3x_1^{exp}$ | $10^3x_1^{Apelblat}$ | $10^3x_1^{CNIBS}$ | $10^3x_1^{AJA}$ |
|---|---|---|---|---|
| 283.15 K | | | | |
| 0.00 | 5.339 | 5.411 | 5.333 | 5.041 |
| 0.30 | 6.582 | 6.621 | 6.649 | 6.478 |
| 0.40 | 6.671 | 6.682 | 6.655 | 6.659 |
| 0.50 | 6.768 | 6.963 | 6.646 | 6.925 |
| 0.60 | 6.856 | 6.928 | 6.826 | 7.438 |
| 0.70 | 7.321 | 7.225 | 7.486 | 8.409 |
| 0.80 | 9.028 | 9.094 | 9.158 | 10.18 |
| 0.90 | 13.57 | 13.90 | 13.15 | 13.39 |
| 1.00 | 23.20 | 23.49 | 23.47 | 19.39 |
| 288.15 K | | | | |
| 0.00 | 5.568 | 5.472 | 5.557 | 5.150 |
| 0.30 | 6.927 | 6.863 | 7.036 | 6.853 |
| 0.40 | 7.223 | 7.100 | 7.278 | 7.134 |
| 0.50 | 7.886 | 7.514 | 7.519 | 7.512 |
| 0.60 | 8.036 | 7.755 | 7.947 | 8.164 |
| 0.70 | 8.365 | 8.416 | 8.861 | 9.332 |
| 0.80 | 10.65 | 10.67 | 10.83 | 11.41 |
| 0.90 | 16.13 | 15.77 | 15.20 | 15.13 |
| 1.00 | 25.26 | 24.82 | 25.82 | 22.06 |
| 293.15 K | | | | |
| 0.00 | 5.706 | 5.635 | 5.697 | 5.377 |
| 0.30 | 7.297 | 7.254 | 7.409 | 7.349 |
| 0.40 | 7.608 | 7.659 | 7.637 | 7.727 |
| 0.50 | 8.373 | 8.205 | 7.995 | 8.214 |
| 0.60 | 8.665 | 8.719 | 8.702 | 9.010 |
| 0.70 | 9.629 | 9.764 | 10.06 | 10.38 |
| 0.80 | 12.55 | 12.40 | 12.62 | 12.78 |
| 0.90 | 18.18 | 17.79 | 17.45 | 17.05 |
| 1.00 | 26.61 | 26.37 | 27.05 | 24.96 |
| 298.15 K | | | | |
| 0.00 | 5.848 | 5.902 | 5.840 | 5.730 |
| 0.30 | 7.746 | 7.806 | 7.870 | 7.982 |
| 0.40 | 8.255 | 8.378 | 8.155 | 8.453 |
| 0.50 | 8.854 | 9.057 | 8.664 | 9.051 |
| 0.60 | 9.556 | 9.844 | 9.648 | 9.992 |
| 0.70 | 11.18 | 11.29 | 11.42 | 11.58 |
| 0.80 | 14.47 | 14.30 | 14.47 | 14.32 |
| 0.90 | 20.03 | 19.93 | 19.59 | 19.17 |
| 1.00 | 27.79 | 28.15 | 28.05 | 28.11 |
| 303.15 K | | | | |
| 0.00 | 6.194 | 6.279 | 6.191 | 6.224 |
| 0.30 | 8.482 | 8.544 | 8.545 | 8.773 |
| 0.40 | 9.138 | 9.284 | 9.044 | 9.336 |
| 0.50 | 9.789 | 10.10 | 9.778 | 10.04 |
| 0.60 | 10.97 | 11.16 | 11.00 | 11.13 |
| 0.70 | 12.98 | 13.00 | 13.04 | 12.95 |
| 0.80 | 16.36 | 16.35 | 16.37 | 16.05 |
| 0.90 | 21.90 | 22.21 | 21.75 | 21.50 |
| 1.00 | 30.29 | 30.20 | 30.38 | 31.51 |
| 308.15 K | | | | |
| 0.00 | 6.842 | 6.779 | 6.840 | 6.882 |
| 0.30 | 9.551 | 9.499 | 9.595 | 9.750 |
| 0.40 | 10.49 | 10.41 | 10.43 | 10.40 |
| 0.50 | 11.49 | 11.37 | 11.49 | 11.22 |
| 0.60 | 13.01 | 12.69 | 13.01 | 12.46 |
| 0.70 | 15.28 | 14.92 | 15.27 | 14.50 |
| 0.80 | 18.52 | 18.56 | 18.72 | 17.98 |
| 0.90 | 24.39 | 24.61 | 24.09 | 24.05 |
| 1.00 | 32.43 | 32.53 | 32.55 | 35.16 |
| 313.15 K | | | | |
| 0.00 | 7.379 | 7.420 | 7.375 | 7.736 |
| 0.30 | 10.66 | 10.72 | 10.76 | 10.95 |
| 0.40 | 11.94 | 11.82 | 11.74 | 11.68 |
| 0.50 | 12.85 | 12.91 | 12.95 | 12.60 |
| 0.60 | 14.63 | 14.47 | 14.63 | 13.99 |
| 0.70 | 17.17 | 17.07 | 17.09 | 16.27 |
| 0.80 | 20.45 | 20.92 | 20.78 | 20.13 |
| 0.90 | 26.81 | 27.13 | 26.39 | 26.85 |
| 1.00 | 34.83 | 35.18 | 35.00 | 39.07 |
| 318.15 K | | | | |
| 0.00 | 8.240 | 8.226 | 8.232 | 8.832 |
| 0.30 | 12.41 | 12.26 | 12.59 | 12.41 |
| 0.40 | 14.05 | 13.55 | 13.80 | 13.22 |
| 0.50 | 15.28 | 14.78 | 15.17 | 14.24 |
| 0.60 | 16.79 | 16.56 | 16.98 | 15.77 |
| 0.70 | 19.44 | 19.47 | 19.56 | 18.29 |
| 0.80 | 23.39 | 23.41 | 23.42 | 22.54 |
| 0.90 | 29.73 | 29.76 | 29.39 | 29.91 |
| 1.00 | 38.64 | 38.19 | 38.84 | 43.25 |
| 323.15 K | | | | |
| 0.00 | 9.249 | 9.229 | 9.248 | 10.23 |
| 0.30 | 14.12 | 14.20 | 14.13 | 14.19 |
| 0.40 | 15.25 | 15.68 | 15.27 | 15.07 |
| 0.50 | 16.80 | 17.06 | 16.70 | 16.17 |
| 0.60 | 18.66 | 18.99 | 18.78 | 17.84 |
| 0.70 | 21.93 | 22.13 | 21.87 | 20.59 |
| 0.80 | 26.37 | 26.04 | 26.41 | 25.23 |
| 0.90 | 32.91 | 32.49 | 32.86 | 33.25 |
| 1.00 | 41.53 | 41.59 | 41.55 | 47.68 |

[a] $x_1$ is the experimental solubility; $x_1^{Apelblat}$, $x_1^{CNIBS}$, and $x_1^{AJA}$ are the calculated mole solubility according to the modified Apelblat model, the CNIBS/R-K model, and the Apelblat−Jouyban−Acree model, respectively. $x_2^0$ represents the initial mole fraction of water in the binary aqueous solvent. [b] The standard uncertainty is $u(T)$= 0.1 K, and the relative standard uncertainties $u_r$ are $u_r(P)$ = 0.01, $u_r(x_1)$ = 0.03, and $u_r(x_2^0)$ = 0.001.

results, the solubility value of any temperature point can be calculated, which can be used to control supersaturation and calculate yield. It is useful to the design of the crystallization process of NAG.[29]

## 5. CONCLUSIONS

The PXRD and thermal analysis confirmed that the crystal form was stable during the whole experiment. Using a gravimetric approach, the solubility of NAG in three pure solvents (water, methanol, and *N*,*N*-dimethylformamide) and four binary solvents (water + methanol, water + *n*-propanol, water + DMF, and water + acetonitrile) was measured between 283.15 and 323.15 K. The solubility of NAG in all solvents was found to be enhanced significantly with increasing temperature. The order of the four solvents' mole fraction solubilities at 298.15 K is water + DMF > water + methanol > water + *n*-propanol > water + acetonitrile. It also increases when the solvent polarity and total hydrogen bond donor inclinations of the solvents rise.



https://doi.org/10.1021/acsomega.3c04044
ACS Omega 2023, 8, 47463−47471

Table 5. Experimental and Correlated Solubility of NAG in Water + Acetonitrile at Temperatures from 283.15 to 323.15 K under Atmospheric Pressure ($p$ = 0.1 MPa)[a,b]

| $x_2^0$ | $10^3x_1^{exp}$ | $10^3x_1^{Apelblat}$ | $10^3x_1^{CNIBS}$ | $10^3x_1^{AJA}$ |
|---|---|---|---|---|
| | | 283.15 K | | |
| 0.30 | 0.3450 | 0.3622 | 0.3550 | 0.3466 |
| 0.40 | 1.200 | 1.217 | 1.075 | 1.105 |
| 0.50 | 2.072 | 2.286 | 2.368 | 2.552 |
| 0.60 | 4.414 | 4.305 | 4.348 | 4.798 |
| 0.70 | 7.807 | 7.940 | 7.267 | 7.954 |
| 0.80 | 11.26 | 11.51 | 11.52 | 12.13 |
| 0.90 | 16.80 | 17.06 | 17.20 | 17.08 |
| 1.00 | 23.20 | 23.49 | 22.94 | 21.49 |
| | | 288.15 K | | |
| 0.30 | 0.4447 | 0.4184 | 0.4425 | 0.4071 |
| 0.40 | 1.345 | 1.336 | 1.390 | 1.271 |
| 0.50 | 3.235 | 2.756 | 2.970 | 2.890 |
| 0.60 | 4.669 | 4.944 | 5.199 | 5.370 |
| 0.70 | 8.885 | 8.714 | 8.383 | 8.816 |
| 0.80 | 13.13 | 12.79 | 13.08 | 13.33 |
| 0.90 | 19.09 | 18.68 | 19.41 | 18.64 |
| 1.00 | 25.26 | 24.82 | 25.13 | 23.34 |
| | | 293.15 K | | |
| 0.30 | 0.4961 | 0.4789 | 0.4926 | 0.4729 |
| 0.40 | 1.496 | 1.470 | 1.533 | 1.449 |
| 0.50 | 3.507 | 3.245 | 3.433 | 3.252 |
| 0.60 | 6.270 | 5.641 | 6.207 | 5.982 |
| 0.70 | 9.701 | 9.598 | 9.857 | 9.745 |
| 0.80 | 14.36 | 14.21 | 14.51 | 14.64 |
| 0.90 | 20.66 | 20.46 | 20.29 | 20.38 |
| 1.00 | 26.61 | 26.37 | 26.76 | 25.43 |
| | | 298.15 K | | |
| 0.30 | 0.5513 | 0.5437 | 0.5495 | 0.5435 |
| 0.40 | 1.642 | 1.618 | 1.659 | 1.638 |
| 0.50 | 3.708 | 3.739 | 3.681 | 3.635 |
| 0.60 | 6.743 | 6.396 | 6.687 | 6.635 |
| 0.70 | 10.63 | 10.61 | 10.73 | 10.75 |
| 0.80 | 15.82 | 15.78 | 15.90 | 16.08 |
| 0.90 | 22.20 | 22.40 | 22.00 | 22.30 |
| 1.00 | 27.79 | 28.15 | 27.87 | 27.79 |
| | | 303.15 K | | |
| 0.30 | 0.5994 | 0.6123 | 0.5962 | 0.6184 |
| 0.40 | 1.757 | 1.782 | 1.795 | 1.838 |
| 0.50 | 4.106 | 4.220 | 3.993 | 4.040 |
| 0.60 | 7.238 | 7.210 | 7.295 | 7.329 |
| 0.70 | 11.68 | 11.76 | 11.78 | 11.82 |
| 0.80 | 17.55 | 17.53 | 17.51 | 17.64 |
| 0.90 | 24.31 | 24.53 | 24.19 | 24.43 |
| 1.00 | 30.29 | 30.20 | 30.35 | 30.45 |
| | | 308.15 K | | |
| 0.30 | 0.6441 | 0.6844 | 0.6415 | 0.6970 |
| 0.40 | 1.940 | 1.966 | 1.968 | 2.046 |
| 0.50 | 4.455 | 4.673 | 4.394 | 4.464 |
| 0.60 | 8.046 | 8.083 | 8.029 | 8.064 |
| 0.70 | 12.93 | 13.07 | 12.99 | 12.98 |
| 0.80 | 19.18 | 19.48 | 19.37 | 19.34 |
| 0.90 | 26.95 | 26.86 | 26.63 | 26.79 |
| 1.00 | 32.43 | 32.53 | 32.54 | 33.45 |
| | | 313.15 K | | |
| 0.30 | 0.7824 | 0.7596 | 0.7783 | 0.7785 |
| 0.40 | 2.159 | 2.169 | 2.201 | 2.262 |
| 0.50 | 4.945 | 5.081 | 4.836 | 4.907 |
| 0.60 | 8.902 | 9.014 | 8.920 | 8.840 |
| 0.70 | 14.45 | 14.56 | 14.56 | 14.22 |
| 0.80 | 21.46 | 21.64 | 21.59 | 21.19 |
| 0.90 | 29.45 | 29.40 | 29.14 | 29.40 |
| 1.00 | 34.83 | 35.18 | 34.95 | 36.83 |
| | | 318.15 K | | |
| 0.30 | 0.8323 | 0.8376 | 0.8332 | 0.8623 |
| 0.40 | 2.393 | 2.395 | 2.382 | 2.484 |
| 0.50 | 5.311 | 5.431 | 5.351 | 5.366 |
| 0.60 | 10.06 | 10.00 | 10.02 | 9.657 |
| 0.70 | 16.37 | 16.26 | 16.35 | 15.54 |
| 0.80 | 23.87 | 24.03 | 23.92 | 23.20 |
| 0.90 | 31.88 | 32.18 | 31.87 | 32.29 |
| 1.00 | 38.64 | 38.19 | 38.64 | 40.64 |
| | | 323.15 K | | |
| 0.30 | 0.9334 | 0.9177 | 0.9321 | 0.9476 |
| 0.40 | 2.672 | 2.646 | 2.690 | 2.710 |
| 0.50 | 6.089 | 5.714 | 6.006 | 5.841 |
| 0.60 | 11.06 | 11.05 | 11.18 | 10.51 |
| 0.70 | 18.28 | 18.20 | 18.28 | 16.95 |
| 0.80 | 27.09 | 26.69 | 26.91 | 25.39 |
| 0.90 | 35.49 | 35.21 | 35.65 | 35.49 |
| 1.00 | 41.53 | 41.59 | 41.49 | 44.92 |

[a] $x_1$ is the experimental solubility; $x_1^{Apelblat}$, $x_1^{CNIBS}$, and $x_1^{AJA}$ are the calculated mole solubility according to the modified Apelblat model, the CNIBS/R-K model, and the Apelblat−Jouyban−Acree model, respectively. $x_2^0$ represents the initial mole fraction of water in the binary aqueous solvent. [b] The standard uncertainty is $u(T)$= 0.1 K, and the relative standard uncertainties $u_r$ are $u_r(P)$ = 0.01, $u_r(x_1)$ = 0.04, and $u_r(x_2^0)$ = 0.001.

Table 6. Main Physicochemical Properties of the Five Pure Solvents[28]

| solvent | $\pi^a$ | $\sum\alpha^b$ | $\sum\beta^c$ |
|---|---|---|---|
| water | 1.09 | 1.17 | 0.47 |
| *N*,*N*-dimethylformamide | 0.88 | 0.00 | 0.74 |
| methanol | 0.60 | 0.43 | 0.47 |
| *n*-propanol | 0.52 | 0.37 | 0.48 |
| acetonitrile | 0.75 | 0.07 | 0.35 |

[a] Polarity of the solvent. [b] Summation of the hydrogen bond donor propensities of the solvent. [c] Summation of the hydrogen bond acceptor propensities of the solvent.

The modified Apelblat model, the CNIBS/R-K model, and the Apelblat−Jouyban−Acree model were used to fit the solubility data. The solubility data measured in this experiment can provide basic data for the optimal design and operation of crystallization processes.

## ■ ASSOCIATED CONTENT

### Supporting Information

The Supporting Information is available free of charge at https://pubs.acs.org/doi/10.1021/acsomega.3c04044.

Experimental and correlated solubility of NAG in water + methanol, water + *n*-propanol, water + DMF, and water + acetonitrile at 283.15−323.15 K, correlative with the



https://doi.org/10.1021/acsomega.3c04044
ACS Omega 2023, 8, 47463−47471

modified Apelblat model; experimental and correlated solubility of NAG in water + methanol, water + *n*-propanol, water + DMF, and water + acetonitrile at 283.15−323.15 K, correlative with the CNIBS/R-K model; model parameters, ARD %, and RMSD of water + methanol, water + *n*-propanol, water + DMF, and water + acetonitrile calculated by the modified Apelblat model, CNIBS/R-K model, and Apelblat−Jouyban−Acree model; and results of several models' *F*-tests in the water + methanol binary solvents (PDF)

## AUTHOR INFORMATION


### Corresponding Authors

**Shichao Du** − *School of Pharmaceutical Sciences, Shandong Analysis and Test Center, Qilu University of Technology (Shandong Academy of Sciences), Jinan 250014, P.R. China*; orcid.org/0000-0002-8369-2983; Phone: 86-531-8260-5824; Email: shichao_du@qlu.edu.cn; Fax: 86-531-8296-4889

**Fumin Xue** − *School of Pharmaceutical Sciences, Shandong Analysis and Test Center, Qilu University of Technology (Shandong Academy of Sciences), Jinan 250014, P.R. China*; orcid.org/0000-0002-8097-0108; Phone: 86-531-8260-5824; Email: xuefumin@qlu.edu.cn; Fax: 86-531-8296-4889

### Authors

**Xiaoyu Cao** − *School of Pharmaceutical Sciences, Shandong Analysis and Test Center, Qilu University of Technology (Shandong Academy of Sciences), Jinan 250014, P.R. China*

**Yan Wang** − *School of Pharmaceutical Sciences, Shandong Analysis and Test Center, Qilu University of Technology (Shandong Academy of Sciences), Jinan 250014, P.R. China*

**Jianxing Lu** − *Shandong Runde Biotechnology Co.,Ltd., Taian 271000, P.R. China*

**Qian Zhang** − *Shandong Runde Biotechnology Co.,Ltd., Taian 271000, P.R. China*

**Tao Yuan** − *Shandong Runde Biotechnology Co.,Ltd., Taian 271000, P.R. China*

Complete contact information is available at: https://pubs.acs.org/10.1021/acsomega.3c04044


### Notes

The authors declare no competing financial interest.

## ACKNOWLEDGMENTS

The authors are grateful for the financial support of the Key R&D Program of Shandong Province, China (2021CXGC010811); the Shandong Provincial Natural Science Foundation (ZR2023MB036); the Central Guidance on Local Science and Technology Development Fund of Shandong Province (YDZX2021054); the Jinan Introducing Innovation Team Project (202228033); the Science, Education, and Industry Integration Technology Innovation Project (2022PY065); and the Talent Research Project of Qilu University of Technology (2023RCKY076).

## REFERENCES


(1) Chen, J. K.; Shen, C. R.; Liu, C. L. N-Acetylglucosamine: Production and Applications. *Mar. Drugs.* **2010**, *8*, 2493−2516.

(2) Gaderer, R.; Seidl-Seiboth, V.; de Vries, R. P.; Seiboth, B.; Kappel, L. N-acetylglucosamine, the building block of chitin, inhibits growth of Neurospora crassa. *Fungal. Genet. Biol.* **2017**, *107*, 1−11.

(3) Hulikova, K.; Svoboda, J.; Benson, V.; Grobarova, V.; Fiserova, A. N-acetyl-D-glucosamine-coated polyamidoamine dendrimer promotes tumor-specific B cell responses via natural killer cell activation. *Int. Immunopharmacol.* **2011**, *11*, 955−961.

(4) Hirano, T.; Aoki, M.; Kadokura, K.; Kumaki, Y.; Hakamata, W.; Oku, T.; Nishio, T. Heterodisaccharide 4-O-(N-acetyl-beta-D-glucosaminyl)-D-glucosamine is an effective chemotactic attractant for Vibrio bacteria that produce chitin oligosaccharide deacetylase. *Lett. Appl. Microbiol.* **2011**, *53*, 161−166.

(5) Azofeifa, D. E.; Arguedas, H. J.; Vargas, W. E. Optical properties of chitin and chitosan biopolymers with application to structural color analysis. *Opt. Mater.* **2012**, *35*, 175−183.

(6) Onuki, K.; Sugiyama, H.; Ishige, K.; Kawamoto, T.; Ota, T.; Ariizumi, S.; Yamato, M.; Kadota, S.; Takeuchi, K.; Ishikawa, A.; Onodera, M.; Onizawa, K.; Yamamoto, M.; Miyoshi, E.; Shoda, J. Expression of N-acetylglucosaminyltransferase V in the subserosal layer correlates with postsurgical survival of pathological tumor stage 2 carcinoma of the gallbladder. *J. Gastroenterol.* **2014**, *49*, 702−714.

(7) Kubomura, D.; Ueno, T.; Yamada, M.; Tomonaga, A.; Nagaoka, I. Effect of N-acetylglucosamine administration on cartilage metabolism and safety in healthy subjects without symptoms of arthritis: A case report. *Exp. Ther. Med.* **2017**, *13*, 1614−1621.

(8) Pizzolatti, A. L. A.; Gaudig, F.; Seitz, D.; Roesler, C. R. M.; Salmoria, G. V. Glucosamine Hydrochloride and N-Acetylglucosamine Influence the Response of Bovine Chondrocytes to TGF-$\beta$3 and IGF in Monolayer and Three-Dimensional Tissue Culture. *Tissue. Eng. Regen. Med.* **2018**, *15*, 781−791.

(9) Ciszewicz, M.; Wu, G.; Tam, P.; Polubinska, A.; Bre Borowicz, A. Glucose but not N-acetylglucosamine accelerates in vitro senescence of human peritoneal mesothelial cells. *Int. J. Artif. Organs.* **2011**, *34*, 489−494.

(10) Hesketh, G. G.; Dennis, J. W. N-acetylglucosamine: more than a silent partner in insulin resistance. *Glycobiology.* **2017**, *27*, 595−598.

(11) Sun, Y.; Zhang, J.; Wu, S.; Shujun, W. Preparation of D-glucosamine by hydrolysis of chitosan with chitosanase and $\beta$-D-glucosaminidase. *Int. J. Biol. Macromol.* **2013**, *61*, 160−163.

(12) Liu, Z.; Yin, Q.; Zhang, H.; Gong, J. Investigation of the Crystallization of Disodium 5′-Inosinate in a Water + Ethanol System: Solubility, Nucleation Mechanism, and Crystal Morphology. *Ind. Eng. Chem. Res.* **2014**, *53*, 8913−8919.

(13) Apelblat, A.; Manzurola, E. Solubilities ofo-acetylsalicylic, 4-aminosalicylic, 3,5-dinitrosalicylic, andp-toluic acid, and magnesium-DL-aspartate in water fromT = (278 to 348) K. *J. Chem.Thermodyn.* **1999**, *31*, 85−91.

(14) Acree, W. E. Mathematical representation of thermodynamic properties: Part 2. Derivation of the combined nearly ideal binary solvent (NIBS)/Redlich-Kister mathematical representation from a two-body and three-body interactional mixing model. *Thermochim. Acta* **1992**, *198*, 71−79.

(15) Pabba, S.; Kumari, A.; Ravuri, M. G.; Thella, P. K.; Satyavathi, B.; Shah, K.; Kundu, S.; Bhargava, S. K. Experimental determination and modelling of the co-solvent and antisolvent behaviour of binary systems on the dissolution of pharma drug; L-aspartic acid and thermodynamic correlations. *J. Mol. Liq.* **2020**, *314*, 113657. DOI: 10.1016/j.molliq.2020.113657

(16) Ouyang, J.; Zhang, Y.; Na, B.; Liu, Z.; Zhou, L.; Hao, H. Solubility Determination of Nicotinamide and Its Application for the Cocrystallization with Benzoic Acid. *J. Chem. Eng. Data* **2018**, *63*, 4157−4165.

(17) Qi, R.; Wang, J.; Ye, J.; Hao, H.; Bao, Y. The solubility of cefquinome sulfate in pure and mixed solvents. *Front. Chem. Sci. Eng.* **2016**, *10*, 245−254.

(18) Fang, J.; Zhang, M.; Zhu, P.; Ouyang, J.; Gong, J.; Chen, W.; Xu, F. Solubility and solution thermodynamics of sorbic acid in eight pure organic solvents. *J. Chem. Thermodyn.* **2015**, *85*, 202−209.

(19) Gao, Z.; Lin, J.; Shi, P.; Cen, Z.; Li, Z.; Han, D.; Gong, J. Solubility Measurement and Data Correlation of 4-Chlorophenoxyacetic Acid in 13 Monosolvents at Temperatures from 283.15 to 328.15 K. *J. Chem. Eng. Data* **2021**, *66*, 2561−2567.

(20) Ma, J.; Liang, J.; Han, J.; Zheng, M.; Zhao, H. Solubility Modeling and Solvent Effect for Flubendazole in 12 Neat Solvents. *J. Chem. Eng. Data* **2019**, *64*, 1237−1243.
(21) Wu, Y.; Zhou, L.; Zhang, X.; Gong, J.; Hao, H.; Yin, Q.; Wang, Z. Determination and Correlation of the Solubility of Acetylpyrazine in Pure Solvents and Binary Solvent Mixtures. *J. Solution Chem.* **2018**, *47*, 950−973.
(22) Yang, Y.; Zhou, L.; Wang, C.; Li, Y.; Huang, Y.; Yang, W.; Hou, B.; Yin, Q. Solubility and Thermodynamic Properties of A Hexanediamine Derivative in Pure Organic Solvents and Nonaqueous Solvent Mixtures. *J. Solution Chem.* **2018**, *47*, 1740−1767.
(23) Barzegar-Jalali, M.; Jouyban-Gharamaleki, A. A general model from theoretical cosolvency models. *Int. J. Pharmaceut.* **1997**, *152*, 247−250.
(24) Zhao, X.; Farajtabar, A.; Zhao, H.; Han, G. Solubility and Solvent Effect of Acetamiprid in Thirteen Pure Solvents and Aqueous Solutions of Ethanol. *J. Chem. Eng. Data* **2019**, *64*, 3505−3513.
(25) Borra, A.; Kosuru, R. K.; Bharadwaj, R.; Satyavathi, B. Measurement and modeling of solubility of furan 2-carboxylic acid in mono and binary systems. *J. Mol. Liq.* **2021**, *326*, 115271, DOI: 10.1016/j.molliq.2020.115271.
(26) Long, B.; Xia, Y.; Deng, Z.; Ding, Y. Understanding the enhanced solubility of 1,3-benzenedicarboxylic acid in polar binary solvents of (acetone + water) at various temperatures. *J.Chem. Thermodyn.* **2017**, *105*, 105−111.
(27) Zorrilla-Veloz, R. I.; Stelzer, T.; López-Mejías, V. Measurement and Correlation of the Solubility of 5-Fluorouracil in Pure and Binary Solvents. *J. Chem. Eng. Data* **2018**, *63*, 3809−3817.
(28) Gu, C. H.; Li, H.; Gandhi, R. B.; Raghavan, K. Grouping solvents by statistical analysis of solvent property parameters: implication to polymorph screening. *Int. J. Pharm.* **2004**, *283*, 117−125.
(29) Zhao, R.; Wan, Y.; Zhang, P.; Wu, N.; Sha, J.; Li, T.; Ren, B. Measurement and modeling correlation of capecitabine solubility in n-hexane + ethyl acetate and n-heptane + ethyl acetate at various temperatures. *J. Mol. Liq.* **2019**, *295*, 111716, DOI: 10.1016/j.molliq.2019.111716.



https://doi.org/10.1021/acsomega.3c04044
*ACS Omega* 2023, 8, 47463−47471